TauCstF-64 Mediates Correct mRNA Polyadenylation and Splicing of Activator and Repressor Isoforms of the Cyclic AMP-Responsive Element Modulator (CREM) in Mouse Testis 1

Authors: Grozdanov, Petar N., Amatullah, Atia, Graber, Joel H., and MacDonald, Clinton C.

Source: Biology of Reproduction, 94(2)

Published By: Society for the Study of Reproduction

URL: https://doi.org/10.1095/biolreprod.115.134684

BIOLOGY OF REPRODUCTION (2016) **94**(2):34, 1–12
Published online before print 23 December 2015.
DOI 10.1095/biolreprod.115.134684

TauCstF-64 Mediates Correct mRNA Polyadenylation and Splicing of Activator and Repressor Isoforms of the Cyclic AMP-Responsive Element Modulator (CREM) in Mouse Testis[1]

Petar N. Grozdanov,[3] Atia Amatullah,[3] Joel H. Graber,[4] and Clinton C. MacDonald[2,3]

[3]*Department of Cell Biology and Biochemistry, Texas Tech University Health Sciences Center, Lubbock, Texas*
[4]*Center for Genome Dynamics, The Jackson Laboratory, Bar Harbor, Maine*

ABSTRACT

Spermatogenesis is coordinated by the spatial and temporal expression of many transcriptional and posttranscriptional factors. The cyclic AMP-responsive element modulator (CREM) gene encodes both activator and repressor isoforms that act as transcription factors to regulate spermiogenesis. We found that the testis-expressed paralog of CstF-64, tauCstF-64 (gene symbol *Cstf2t*), is involved in a polyadenylation site choice switch of *Crem* mRNA and leads to an overall decrease of the *Crem* mRNAs that are generated from internal promoters in *Cstf2t*$^{-/-}$ mice. More surprisingly, loss of tauCstF-64 also leads to alternative splicing of *Crem* exon 4, which contains an important activation domain. Thus, testis-specific CREMtau2 isoform protein levels are reduced in *Cstf2t*$^{-/-}$ mice. Consequently, expression of 15 CREM-regulated genes is decreased in testes of *Cstf2t*$^{-/-}$ mice at 25 days postpartum. These effects might further contribute to the infertility phenotype of these animals. This demonstrates that tauCstF-64 is an important stage-specific regulator of *Crem* mRNA processing that modulates the spatial and temporal expression of downstream stage-specific genes necessary for the proper development of sperm in mice.

alternative splicing, cleavage and polyadenylation, CREM, spermatogenesis, τCstF-64

INTRODUCTION

The most common form of male infertility is idiopathic impairment of spermatogenesis [1–3]. Many idiopathic cases of male infertility are likely caused by autosomal recessive genes, including those involved in transcriptional and posttranscriptional control of gene expression [4–7]. During spermatogenesis, the expression of specialized transcription factors ensures that the complex processes of male gamete formation will be accomplished properly. One of those transcription factors is the cyclic AMP-responsive element modulator (CREM; gene symbol: *Crem*), which plays a central role in the control of spermatogenesis [8–10]. While CREM is expressed in many tissues, in testis it interacts with tissue-specific factors such as the activator of CREM in testis (ACT; gene symbol *Fhl5*) that support its central function to promote spermatogenesis [11]. CREM and ACT expression are spatially and temporally correlated during spermatogenesis [12], making correct expression of these transcription factors critical for male fertility [13].

In the adult mouse testis, the major protein isoform of CREM is called CREMτ [14]. During testicular development, CREMτ expression increases strikingly between 13 and 14 days postpartum (dpp). During that time period, many alternatively spliced and polyadenylated mRNA forms become prominent [14–19]. Some *Crem* mRNA isoforms also initiate from alternative transcription start sites in male germ cells [20]. One CREM protein isoform, the transcriptional repressor S-CREM, results from use of an internal translational start site [21]. CREMτ functions as an activator of gene transcription of stage-specific genes required for male gamete formation [9]. Two additional isoforms, CREMτ1 and CREMτ2, are produced by alternative splicing of exons 4 and 7 in different tissues [14, 15, 22, 23]; these isoforms are also transcriptional activators. Consistent with these roles, male mice deficient for the *Crem* gene lack spermatozoa, have reduced seminiferous tubule diameter, and halt spermatogenesis at early stages of round spermatid formation [24].

Alternative polyadenylation is a major contributor to the isoform diversity of the *Crem* gene. A developmental switch in polyadenylation site choice during spermatogenesis increases the stability of the *Crem* mRNA by truncating control elements in its 3′ untranslated region (UTR) [19]. One key cleavage and polyadenylation protein, the RNA-binding subunit (CstF-64; gene symbol *Cstf2* [25, 26]) of the cleavage stimulation factor (CstF) has a testis-expressed paralog, τCstF-64 (gene symbol *Cstf2t* [27, 28]), necessitated by meiotic silencing of its X-linked paralog *Cstf2* [29]. In somatic cells, CstF-64 acts to bind to the downstream sequence element (DSE) during early recognition steps of polyadenylation so that cooperation between the CstF complex and the cleavage and polyadenylation specificity factor (CPSF) can direct cleavage and subsequent poly(A) addition to occur at the favored site [30, 31]. In male germ cells, τCstF-64 appears to replace the functionality of CstF-64 during meiosis and subsequent spermiogenesis [25, 32–34]. Thus, male mice lacking τCstF-64 are infertile, demonstrating low sperm counts and severe abnormalities in sperm morphology and motility [35–37]. These abnormalities appear to be due to large-scale alterations in genome expression [35, 38], suggesting that τCstF-64

[1]Research reported in this publication was supported by the Eunice Kennedy Shriver National Institute of Child Health and Human Development of the National Institutes of Health under award number R01HD037109. Additional support was from the Laura W. Bush Institute for Women's Health. The content is solely the responsibility of the authors and does not necessarily represent the official views of the National Institutes of Health.
[2]Correspondence: Clinton C. MacDonald, Department of Cell Biology and Biochemistry, Texas Tech University Health Sciences Center, 3601 4th St., Lubbock, Texas 79430-6540. E-mail: clint.macdonald@ttuhsc.edu

Received: 18 August 2015.
First decision: 25 September 2015.
Accepted: 17 December 2015.

eISSN: 1529-7268 http://www.biolreprod.org
ISSN: 0006-3363

regulates multiple levels of gene expression in these animals beyond mRNA biogenesis.

We report here on experiments to determine how loss of τCstF-64 leads to male infertility through its action on important spermatogenic regulators like *Crem*. Overall, loss of τCstF-64 resulted in reduced expression of a specific CREM activator protein isoform (CREMτ2) in mouse testes. Analysis of high-throughput sequencing of regions adjacent to polyadenylation sites (A-seq) revealed polyadenylation site switching in *Crem* mRNA to a more distal site in *Cstf2t*$^{-/-}$ mouse testes. However, changes in polyadenylation were not sufficient to account fully for the altered CREM protein expression in *Cstf2t*$^{-/-}$ mice. High-throughput cDNA sequencing (RNA-seq) and confirmatory quantitative RT-PCR revealed that additional reductions could be accounted for by reduced *Crem* mRNA isoforms initiating from internal promoters. Strikingly, *Crem* gene transcripts that omitted exon 4 were consistently reduced in knockout animals, suggesting that τCstF-64 was involved, either directly or indirectly, in exon 4 exclusion in mice. Consistent with reduced CREMτ2 expression, 15 of 58 genes that were reported to be directly regulated by CREM were down-regulated at least 2-fold in *Cstf2t*$^{-/-}$ mice. Thus, τCstF-64 is important for the stage-specific regulation of *Crem* isoforms that further regulate the correct expression of downstream stage-specific genes required for the proper development of sperm in mice.

MATERIALS AND METHODS

Animal Use and Isolation of Seminiferous Tubules

Wild-type and *Cstf2t*$^{-/-}$ mice in a C57BL/6 (Charles River) background were bred in-house. Except where noted, all mice were 25 dpp [38]. All animals and testis tissues used in the study were obtained according to protocols approved by the Institutional Animal Care and Use Committee at the Texas Tech University Health Sciences Center in accordance with the National Institutes of Health animal welfare guidelines.

Seminiferous tubules were isolated as follows: a small incision was made in the tunica albuginea of the testis, and the contents (mainly seminiferous tubules) were gently collected in ~5 ml [34] of ice-cold Dulbecco Phosphate-Buffered Saline (DPBS; Life Technologies) supplemented with phenylmethanesulfonyl fluoride (PMSF). The contents were vigorously shaken, breaking apart the tissue. Tissue parts were allowed to settle at unit gravity for 5 min on ice, and the supernatant (containing mainly Leydig cells) was aspirated. The procedure was repeated three times. After the final settlement, the tissue was spun briefly in a microcentrifuge at ~500 × *g*. The obtained seminiferous tubules were used to isolate either total RNA or protein.

Protein Isolation and Immunoblots

Seminiferous tubules from one animal were lysed in either 250 µl extraction buffer (DPBS, 0.5 % Triton X-100 [v/v], 2 mM PMSF, 0.02% NaN_3) or RIPA buffer (50 mM Tris-HCl, pH 8.8, 150 mM NaCl, 0.1% sodium dodecyl sulfate, 0.5% deoxycholate, 0.5% NP-40), briefly sonicated, and incubated on ice for 10 min. Lysates were spun down for 10 min at 400 × *g* at 4°C for 10 min. Equal amounts of protein from wild-type and *Cstf2t*$^{-/-}$ animals were loaded on precast NuPAGE Novex 4%–12% Bis-Tris Gels (Life Technologies), followed by a semidry transfer to polyvinylidene fluoride membranes. Membranes were incubated with primary antibody as indicated, followed by the appropriate secondary antibody conjugated to horseradish peroxidase. The following primary antibodies were used: rabbit anti-CREM (Santa Cruz Biotechnology; X-12, sc-440, used at a dilution of 1:500), rabbit anti-SRp40 (Millipore; 06-1365, dilution of 1:1000), and rabbit anti-DAZAP1 (Bethyl Laboratory; A303-985A-T, dilution of 1:2000). Mouse anti-CstF-64 (3A7) and mouse anti-τCstF-64 (6A9) were used as described [25, 32]. The E7 anti-β-tubulin monoclonal antibody (developed by Michael Klymkowsky and obtained from the Developmental Studies Hybridoma Bank) was a gift from Daniel Webster and used at a dilution of 1:1000. Anti-SRSF10 (formerly SRp38, dilution of 1:1000) was a gift from Dr. James L. Manley [39].

RNA Isolation and RNA-Seq

RNA-seq was carried out as described previously [34]. Total RNA from seminiferous tubules from one animal was extracted using 1 ml TRIzol reagent (Life Technologies). Quantity of the isolated total RNA was determined by spectrophotometric measurement using the NanoDrop device. The quality of the RNA was determined using standard 1% agarose gel electrophoresis. For the RT-PCR and quantitative RT-PCR (qRT-PCR), the RNA was treated with RQ1 (RNA Qualified) RNase-Free DNase (Promega) as recommended. RNA-seq libraries from three wild-type and three knockout animals were prepared using Illumina's TruSeq RNA Sample Preparation Kits v2 (Illumina Inc.). Briefly, 4 µg of total RNA was poly(A)-selected, followed by generation of double-stranded cDNA. Adapters were ligated, and resulting fragments were amplified by limited number of PCR cycles. RNA-seq libraries were sequenced on HiSeq 2000 platform with 90-nucleotide coverage of each end (PE90). Over 41 million individual sequences from each library were collected with a Q20% larger than 97%.

A-Seq Library Preparation

A-seq was carried out essentially as described previously [34, 40]. Briefly, 40 µg of total RNA were used to isolate the poly(A)$^+$ fraction using the Dynabeads mRNA direct Kit (Life Technologies). Poly(A)-selected RNA was partially digested with three different concentrations of RNase I (Ambion), reselected for poly(A), and the 5′ ends were phosphorylated on the Dynabeads. Subsequently, RNAs were eluted and 3′ ends blocked using cordycepin 5′-triphosphate (Sigma) and *Escherichia coli* poly(A) polymerase (New England Biolabs). Simultaneously, the RNAs were treated with RQ1 RNase-Free DNase (Promega). After phenol-chloroform extraction and ethanol precipitation, a 5′ adapter (RA5; Illumina) was ligated. RNAs were reverse transcribed to complementary DNA using a ^{32}P-labeled primer. The cDNAs were resolved on 5% denaturing polyacrylamide gel, and the cDNAs between ~120 and ~150 nucleotides (nt) were isolated. PCR was performed with primers adapters similar to the TruSeq Small RNA Sample Preparation Kit (Illumina). The resulting cDNA libraries representing the 3′ ends of polyadenylated RNAs were sequenced on Illumina platform with 50-nucleotide coverage (SE50). The obtained reads were strand specific and coincided with the sense strand of the mRNAs.

HITS-CLIP Library Preparation

Cross-linking and immunoprecipitation combined with high-throughput sequencing (HITS-CLIP) was performed exactly as previously described [41] except using both the CstF-64-specific 3A7 and τCstF-64-specific 6A9 monoclonal antibodies [25].

Bioinformatics

RNA-seq reads obtained from each biological replicate were independently aligned on the mouse reference genome (Mouse Genome v37.2, MGSC v37, mm9) using the SeqMan NGen v10 software (DNASTAR Inc.). The assembly files generated by SeqMan NGen were used to identify the differentially expressed genes (2-fold change) using the QSeq part of ArrayStar package (DNASTAR).

A-seq data were initially processed with the FASTQC package [42] to identify the nature of the typical spacing of 5′ and 3′ adapter sequences. Custom in-house software was then used to remove sequences that contained only the adapter with no inserts. As the amount of sequence between adapters was variable, a common target length of 24 nt anchored on the putative poly(A) site was chosen as a compromise between retaining genomic uniqueness and retention of the largest possible number of sequences. Sequences as short as 16 nt were also kept but then collapsed to a matching 24-nt tag. There was also variability across samples noted in the presence of the 3′ adapter, indicating the precise site of poly(A) addition. In some libraries, a majority (>75%) of the sequences failed to show the adapter. However, analysis of the sequence content across the whole library suggested that the adapter sequence was immediately or very near the downstream of the end of the sequenced insert. These tags were labeled ''near'' rather than ''exact'' and subsequently assigned to the nearest ''exact'' poly(A) site after genomic alignment. To reduce computation time, the number of each tag was noted, and a working file was generated with only one representative copy of each putative tag. Representative sequences were aligned to a database of reference repetitive element sequences such that those sequences that matched the repetitive elements could be removed from downstream analysis. The remaining representative tags were then aligned to the mouse genome GRC v38 with BLAT [43]. Tags were

assigned to the nearest properly oriented exon according to the Ensembl mouse v70 annotations [44].

HITS-CLIP sequence data was processed initially by the Beijing Genome Institute by removing low-quality sequences, identifying 5′ and 3′ adapters, extracting the insert sequence between these, filtering based on a minimum length, and reducing the file to only single instances of each unique sequence, retaining the number of times each sequence as part of its annotation. The resulting file was aligned to a database of reference repetitive element sequences such that those sequences that matched the repetitive elements could be removed from downstream analysis. Sequences that passed this filtering were then aligned to the mouse genome GRC v38 with BLAT [43]. Empirical analysis revealed that sequences could be grouped based on common 3′-end positions, and that position was subsequently used to identify and quantify putative binding site usage. Genomic alignments were further carried out and compared with the PIPE-CLIP analysis software [45], using standard parameters.

Analysis of Alternative Splicing

We manually created 40-nt-long query sequences that represented the exon-exon junctions in the ENSMUST00000150235 transcript (Tx1; see Fig. 3). Using a local BLAST engine, RNA-seq data sets were converted to a custom searchable library. Exon-exon junction sequences were used to query the custom data sets, and the number of raw hits was recorded. Raw hits were normalized using RPKM normalization method [46, 47], using 40 nt as length for the gene, consistently between the samples. Average RPKM was calculated, and a two-tailed Student *t*-test between similar pairs was performed to show statistical significance.

Reverse Transcription, RT-PCR, and qRT-PCR

Complementary DNA for RT-PCR and qRT-PCR was prepared from 80 ng of total RNA using SuperScript VILO MasterMix (Life Technologies) to verify gene expression levels. To confirm the cleavage and polyadenylation site choice in wild-type and *Cstf2t*$^{-/-}$ mice, we used oligo(dT)-primed RNA. RT-PCR was performed using EmeraldAmp GT PCR Master Mix (Clontech) for 25–30 cycles with exon-specific primers as indicated (Supplemental Table S1; Supplemental Data are available online at www.biolreprod.org). PCR products were resolved on 2% agarose gel electrophoresis stained with ethidium bromide and visualized with UV-transilluminator. Percent-spliced-in (PSI) values were calculated by measuring the (relative intensity of the PCR product including exon 4) divided by (intensity of the PCR product including exon 4 plus the intensity of the PCR product excluding exon 4) multiplied by 100%. Background intensity value was subtracted from the intensity of the PCR products; qRT-PCR was performed using Power SYBR Green PCR Master Mix (Life Technologies) on the QuantStudio 12K Flex Real-Time PCR System in triplicate. The relative expression was calculated using the comparative C_t method using 18S rRNA as a reference for the gene expression study and *Glul* gene to normalize relative usage of cleavage and polyadenylation site choice of *Crem* gene [48].

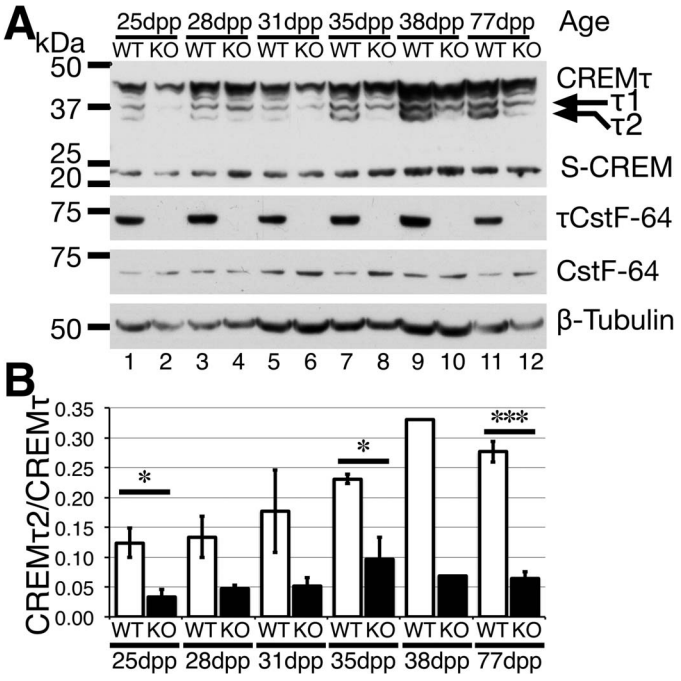

FIG. 1. Expression of CREM and CREMτ protein isoforms decreases in testes of *Cstf2t*$^{-/-}$ mice. **A**) Western blot analysis of CREMτ CREMτ1/2, S-CREM, τCstF-64, and CstF-64 expression in wild-type (lanes 1, 3, 5, 7, 9, 11) and *Cstf2t*$^{-/-}$ (lanes 2, 4, 6, 8, 10, 12) mouse testes at 25 (lanes 1 and 2), 28 (lanes 3 and 4), 31 (lanes 5 and 6), 35 (lanes 7 and 8), 38 (lanes 9 and 10), and 77 (lanes 11 and 12) dpp. Molecular weight standards (in kDa) are shown on left. **B**) Densitometry was done to compare the intensity of the darkest band (CREMτ) to CREMτ2 (as first normalized to β-tubulin) to demonstrate the relative reduction of CREMτ2 in *Cstf2t*$^{-/-}$ mouse seminiferous tubules. A single asterisk (*) denotes $P < 0.05$, and three asterisks (***) denote $P < 0.001$ by a one-tailed Student *t*-test of three separate animals.

RESULTS

CREMτ Protein Isoforms Are Reduced in the Seminiferous Tubules of Cstf2t$^{-/-}$ Mice

The balance of full-length CREMτ with its cognate protein isoforms is critical for progression through spermatogenesis [49]. These isoforms are controlled in part by hormonal regulation of selection among *Crem* 3′ polyadenylation sites [11, 19]. Therefore, we examined CREM protein expression in lysates from seminiferous tubules from wild-type and *Cstf2t*$^{-/-}$ mice of 25, 28, 31, 35, 38, and 77 dpp (Fig. 1A). The CREMτ protein was expressed in testes of wild-type and *Cstf2t*$^{-/-}$ mice of all ages (Fig. 1A). However, the CREMτ2 protein isoform was decreased relative to the major CREMτ isoform in seminiferous tubules from *Cstf2t*$^{-/-}$ mice at all ages (Fig. 1B). The S-CREM translational isoform [21] did not vary consistently between wild-type and *Cstf2t*$^{-/-}$ mouse seminiferous tubules (Fig. 1). This suggests that τCstF-64 supports both expression of CREMτ and expression of specific CREM isoforms in mouse testis but that not all isoforms are affected in the same manner. Consistent with previous reports, CstF-64 expression was increased in the *Cstf2t*$^{-/-}$ mice likely due to posttranscriptional regulation [34, 35, 50]; 25 dpp was chosen for further studies because this age showed critical effects of *Cstf2t* loss while showing the least effects of later stages of germ cell loss (Supplemental Figure S1).

Crem Cleavage/Polyadenylation Switches from Proximal to Distal Sites in Seminiferous Tubules from Cstf2t$^{-/-}$ Mice

Altered CREM protein expression in seminiferous tubules from *Cstf2t*$^{-/-}$ mice suggested changes in *Crem* mRNA processing [10, 49]. To address polyadenylation changes, we constructed a genome-wide library representing 3′-ends formed by cleavage and polyadenylation in the seminiferous tubules of 25-dpp wild-type and *Cstf2t*$^{-/-}$ mice using the A-seq method [40]. Analysis of A-seq indicated that at least 11 cleavage and polyadenylation sites were present for *Crem* in testes of wild-type 25-dpp mice (Fig. 2A). Two of these sites (sites 3 and 8; Fig. 2A) were most prominent. Relative use of sites 3 and 8 differed between wild-type and *Cstf2t*$^{-/-}$ mice: site 3 was used most prominently in wild type mice, while site 8 was used most prominently in *Cstf2t*$^{-/-}$ mice (Fig. 2A). Relative use of each of these sites was confirmed by qRT-PCR (Fig. 2B).

To test whether τCstF-64 might play a direct role in *Crem* polyadenylation, we identified potential RNA binding sites for τCstF-64 by high-throughput sequencing of RNA isolated by cross-linking and immunoprecipitation (HITS-CLIP) using an antibody specific for mouse τCstF-64 [25, 32, 41]. HITS-CLIP did not identify unique τCstF-64 binding sites in the 3′ exon of

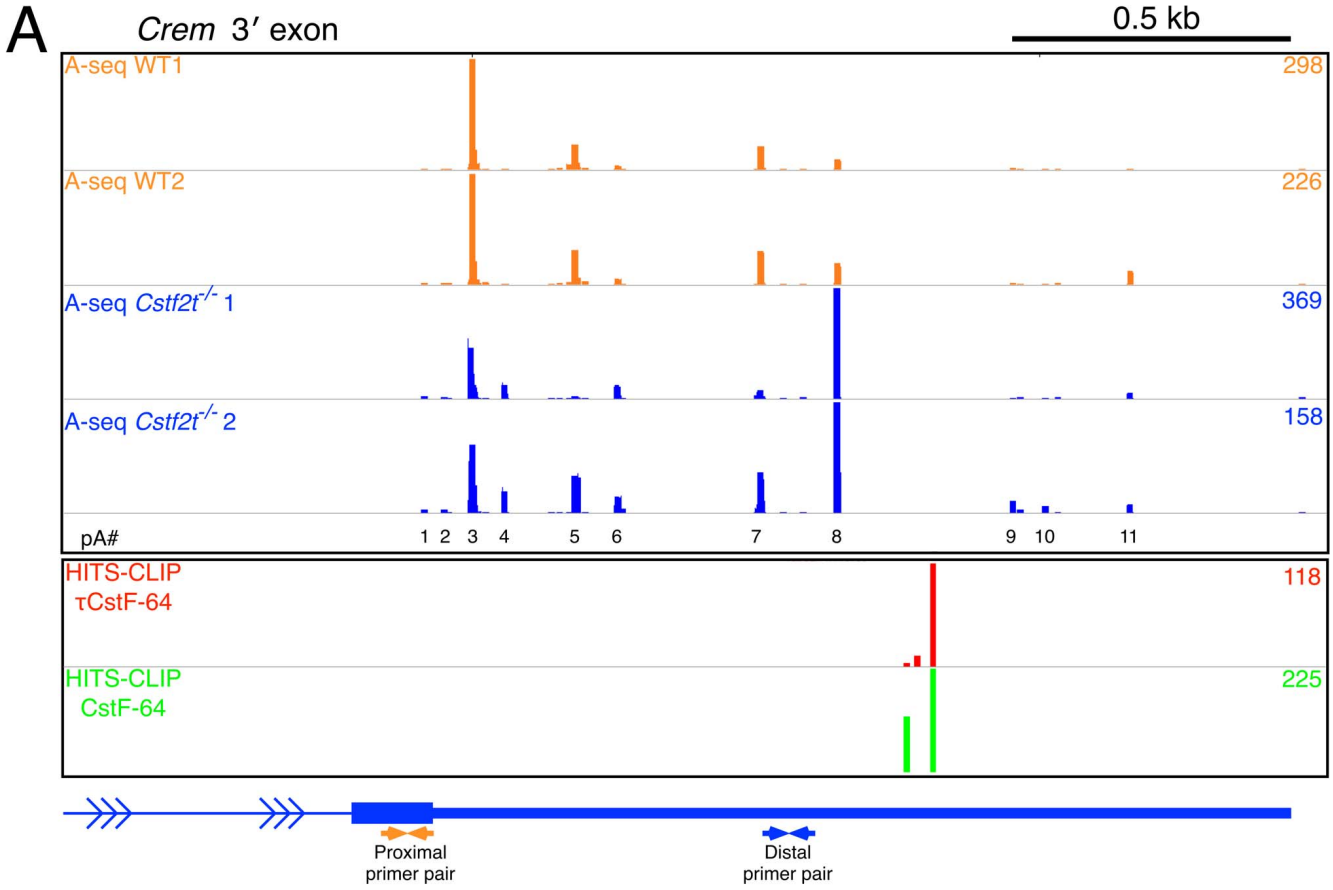

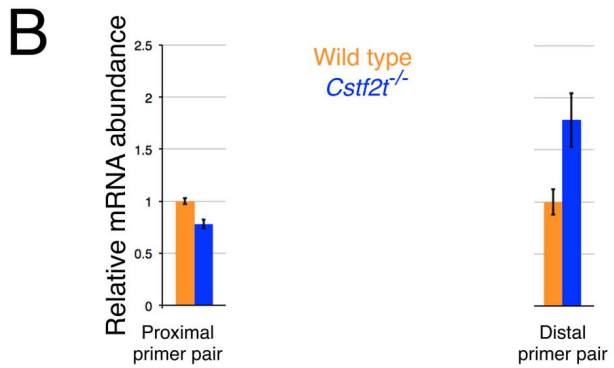

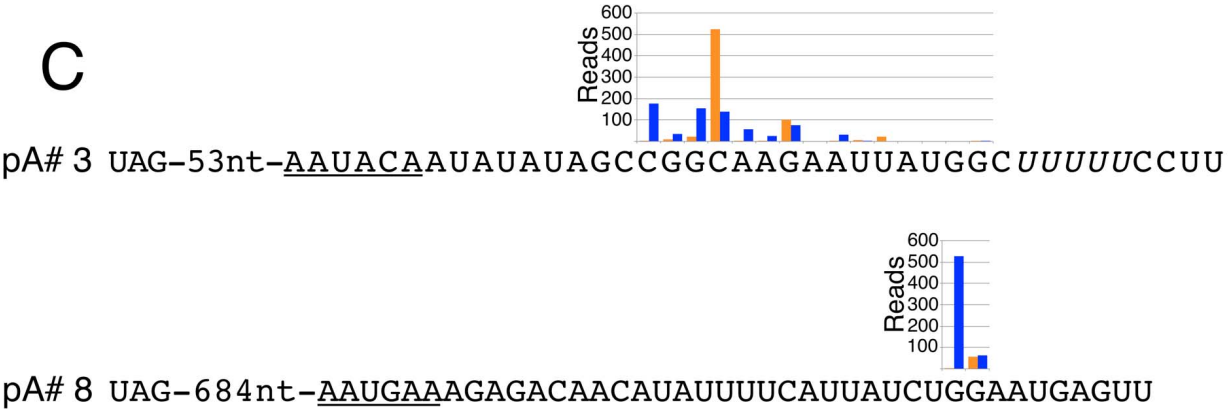

FIG. 2. *Crem* cleavage/polyadenylation sites change in wild-type and *Cstf2t*$^{-/-}$ seminiferous tubules. **A**) A-seq reads representing cleavage/polyadenylation sites mapped on the mouse genome (mm10) from two wild-type (WT1, WT2, top orange bars) or two *Cstf2t*$^{-/-}$ (*Cstf2t*$^{-/-}$ 1, *Cstf2t*$^{-/-}$ 2, middle blue bars) mice. Values in orange (wild type) and blue (*Cstf2t*$^{-/-}$) on right represent the highest number of reads assigned to a specific 3′ cleavage site in the corresponding tracks. Specific polyadenylation sites are designated 1 through 11 (pA#1–11, indicated at bottom). Bottom panels show τCstF-64 (red, top) and CstF-64 (green, bottom) binding sites determined using HITS-CLIP. The last intron and 3′ exon of *Crem* are shown (blue). Distal and proxima

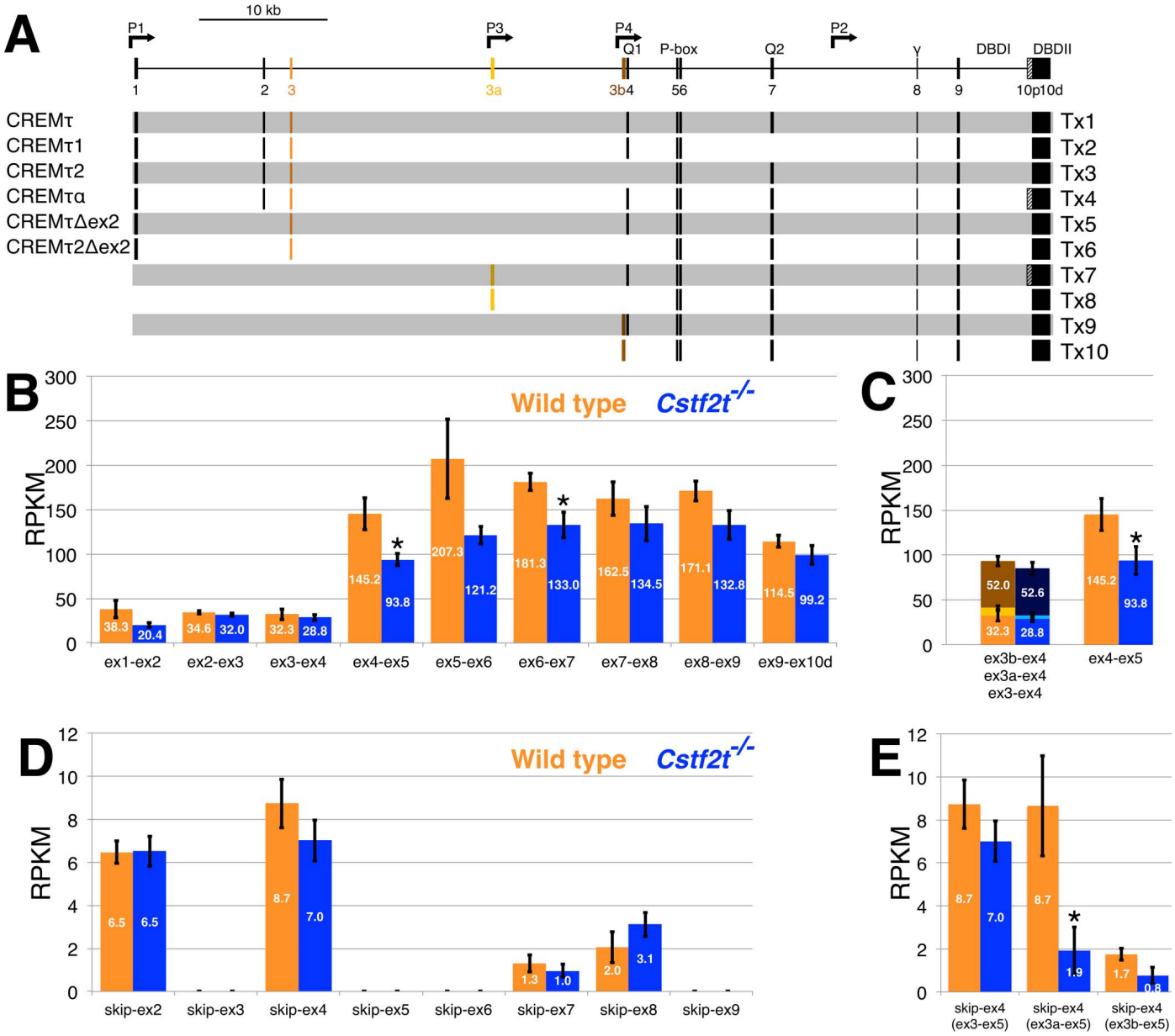

FIG. 3. *Crem* transcript variants expressed in wild-type and *Cstf2t*$^{-/-}$ mouse seminiferous tubules. **A**) Map of the *Crem* gene showing promoters, exons, and introns. Encoded protein isoforms of CREM are shown on left and transcript variants (Tx 1–10) on right. Tx1 corresponds to Ensembl transcript ENSMUST00000150235, Tx7 corresponds to ENSMUST00000154715, and Tx9 corresponds to ENSMUST00000122958. Promoters P1–P4 are shown with their specific location within the gene. Exons numbered 1 through 9 and 10d (distal) encode variants of CREMτ with initiation at P1 corresponding to transcripts 1 to 6 (Tx1–6); mRNA variants splicing at exon 10p (proximal) encode the CREMτα isoform (Tx4). Exons 3a and 3b represent transcripts initiating in promoters P3 (Tx7, Tx8) and P4 (Tx9-10), respectively. Exons 4 and 7 (encoding the glutamine-rich activator domains Q1 and Q2), the P-box (containing a phosphorylation site), the γ domain, and two DNA binding domains (DBDI and DBDII) are indicated at top. **B**) RPKM-normalized RNA-seq data of exon-exon junction for Tx1 in wild-type (in orange) and *Cstf2t*$^{-/-}$ (in blue) mouse testes. The asterisk (*) denotes $P < 0.05$ by a two-tailed Student *t*-test. **C**) RPKM-normalized RNA-seq data of exon-exon junctions ex3–ex4 (Tx1), ex3a–ex4 (Tx7), and ex3b–ex4 (Tx9) in wild-type (in orange, yellow, and brown) and *Cstf2t*$^{-/-}$ (in blue, light blue, and dark blue) mice, respectively. Bar graph on right represents ex4–ex5 taken from **B** for comparative purposes. **D**) RPKM-normalized RNA-seq data of exon-exon junction for transcripts skipping exons 2–9 in wild-type (in orange) and *Cstf2t*$^{-/-}$ (in blue) mouse testes derived from Tx1. **E**) RPKM-normalized RNA-seq data of exon-exon junction for transcripts skipping exon 4 in transcripts initiating in P1 (exon 3), P3 (exon 3a), and P4 (exon 3b) in wild-type (orange) and *Cstf2t*$^{-/-}$ (blue) mouse testes.

l primer pairs used to confirm cleavage and polyadenylation switch in the last exon of *Crem* in **B** are indicated. **B**) Relative mRNA abundance of transcripts terminating at pA#3 and pA#8 in seminiferous tubules from two independent wild-type (orange) and two independent *Cstf2t*$^{-/-}$ (blue) mice as determined by qRT-PCR (primers in Supplemental Table S1). **C**) 3′ cleavage sites, putative polyadenylation signals (underlined), and U-rich downstream sequence elements (italic) for pA#3 and pA#8. A-seq reads corresponding to the sites of poly(A) addition are indicated above the sequences in orange (wild type) and blue (*Cstf2t*$^{-/-}$). Reads represent the sum of the A-seq reads shown in **A** for the two wild-type and two knockout animals, respectively.

Crem in wild-type mouse testes (Fig. 2A). However, it did identify shared τCstF-64/CstF-64 binding sites ~150–175 nt downstream of polyadenylation site 8 (Fig. 2A). The relative strengths of the polyadenylation signals (PAS) at sites 3 and 8 revealed that site 3 is ''stronger'' (i.e., it conforms better to the PAS consensus [51]). Typically, polyadenylation results in addition of poly(A) at one or two closely spaced nucleotides at each site [52]. Further examination of A-seq indicated that loss of τCstF-64 caused the specific sites of poly(A) addition to spread over a broadly spaced range of nucleotides near site 3 (Fig. 2C), a phenomenon we refer to as ''defocusing.'' We saw less evidence of defocusing at site 8 (Fig. 2C). However, we did not see HITS-CLIP evidence supporting binding of either CstF-64 or τCstF-64 to any of the nearby (≤25 nt) GU-rich downstream sequences at site 3 (Fig. 2, A and C).

Many Variant Crem *Transcripts Are Expressed in Mouse Testes*

The Ensembl transcriptome database [44] describes 41 transcript variants for the *Crem* gene, making analysis of the RNA-seq data more complex. In Figure 3A, the transcripts designated Tx1 (which corresponds to ENSMUST00000150235) and Tx4 encode CREMτ and CREMτα [17], respectively. Using Tx1 as a template, we designed 40-nt-long exon-exon junction sequences (20 nt on each side of the junction) for each pair of adjacent exons (e.g., ex1–ex2, ex2–ex3, etc.). We mapped the RNA-seq data from wild-type mice to *Crem* using local BLAST and identified the number of reads that mapped to the exon junctions. In wild-type mice, the highest RPKM observed was 207.3 for the ex5–ex6 junction (Fig. 3B), and the lowest was 32.3 for the ex3–ex4 junction. The decreased number of reads mapped to the *Crem* 5′ end suggested that there are *Crem* transcripts initiating from promoters P3 (exon 3a) and P4 (exon 3b) in our mice. This pattern was seen in both wild-type and *Cstf2t*$^{-/-}$ mice (Fig. 3B). The sum of all of reads mapped to exons 3, 3a, and 3b is approximately equal to the number of reads detected in the 3′ end of *Crem* for ex9–ex10d (Fig. 3, B and C), suggesting that promoters downstream of 3b do not contribute significantly to *Crem* expression in our mice. We did not detect any upstream splicing events involving exon 3a or 3b with exon 3 or 2, consistent with the promoter identification. The reads that mapped to exons 3 and 4 represented 34.6% of the total reads aligned on exon 4, suggesting that the upstream mRNA initiates transcription at P1 (exon 1); 9.7% of the reads mapped to the exon-exon junction between exons 3a and 4, and 55.7% aligned to the nucleotide query covering exons 3b and 4 (Fig. 3C). In summary, we confirmed expression of CREMτ and mRNAs initiating from P1 (Fig. 3A; Tx1–Tx6), P3 (Tx7, Tx8), and P4 (Tx9, Tx10). The most abundant transcripts were those initiating at P4, followed by those initiating at P1 and P3.

The last exon of *Crem* (exon 10; Fig. 3A) contains two alternative 3′-splice acceptor sites. Alternative use of these 3′-splice sites results in two isoforms of CREMτ that differ at their carboxy-termini [12]. CREMτα is encoded by mRNAs that splice to the proximal 3′-splice acceptor in exon 10 (10p in Fig. 3A), and CREMτ is encoded by mRNAs that splice to the distal 3′-splice acceptor (10d). Only 3.88% of the *Crem* mRNA spliced to 10p (CREMτα) in our wild-type mice. The remaining sequences (96.12%) represent mRNAs encoding CREMτ (10d).

The inducible cyclic AMP early repressor (ICER) is another product of *Crem* that results from transcription initiation at promoter P2 between exons 7 and 8 [20]. Surprisingly, we did not detect reads indicating transcriptional initiation at P2 that further included exon 8, indicating that seminiferous tubules in our mice express little or no ICER. However, we did identify a small number of reads that initiate at a promoter P6 downstream of P2. These transcripts likely represent a recently discovered variant of ICER named smICER [53].

Expression of Crem *mRNA Downstream of Exon 4 Is Reduced in* Cstf2t$^{-/-}$ *Mice*

To examine overall expression levels of *Crem* mRNA in the testes of wild-type and *Cstf2t*$^{-/-}$ mice, we compared the abundances of the individual exon-exon junctions. Overall, *Crem* mRNA expression was reduced 1.4-fold in *Cstf2t*$^{-/-}$ mice compared to wild type (ex1–ex2 to ex9–ex10; Fig. 3B). However, when regions of *Crem* downstream of exon 4 (ex4–ex5 to ex9–ex10) were analyzed separately, *Crem* was reduced 1.5-fold. These transcripts initiate at promoters P3 and to a smaller extent P1 (Fig. 3A). Because the transcriptional activation domains Q1 and Q2 of CREM are encoded by exons 4 and 7, this suggests that the activation functions of CREMτ might be reduced in *Cstf2t*$^{-/-}$ mice (Fig. 3B; see also Fig. 1).

Alternatively Spliced mRNA Variants of Crem *in Testes of Wild-Type and* Cstf2t$^{-/-}$ *Mice*

Crem expression is regulated extensively by alternative splicing [14, 15, 22, 23], so we chose to determine whether loss of τCstF-64 affected *Crem* splicing. CREMτ1 (Fig. 3A; Tx2) and CREMτ2 (Tx3) are formed by alternative cassette splicing of exons 4 and 7 of *Crem* [15, 17, 22]. In addition, skipping of exons 2 (Tx5, Tx6) and 8 has been reported [12, 54]. Therefore, we assessed the total number of normalized reads from exons that skipped the immediate downstream exon in *Crem* transcripts in testes of wild-type mice and expressed that as a percentage of the total (Fig. 3, D and E). For example, we created a sequence query that skipped exon 2; for example, the first 20 nt of the query were within the 3′ end of exon 1, and the remaining 20 nt were within the 5′ end of exon 3. We observed that exons 3, 5, 6, and 9 were never excluded from *Crem* transcripts. However, approximately 20% of transcripts excluded exon 4 in wild-type mice (Fig. 3A; Tx3, Tx6, Tx8). Approximately 17% of the mRNAs encoding CREMτ (Tx1) excluded exon 2 (Fig. 3D). Only 0.7% of *Crem* transcripts excluded exon 7 (Tx3), and 1.2% of *Crem* transcripts excluded exon 8. *Crem* transcripts initiating at P3 (Tx7, Tx8) had an approximately equal number of reads that included or excluded exon 4 (Fig. 3, C and E). However, only 3.2% of reads corresponding to Tx9 (initiating at P4) skipped exon 4 (Fig. 3, C and E). Thus, the most abundant transcript produced in the seminiferous tubules of 25-dpp wild-type C57BL/6 mice is Tx9 (55.8%), followed by Tx1 (34.6%).

Crem *Isoforms That Exclude Exon 4 Are Downregulated in* Cstf2t$^{-/-}$ *Mice*

To assess differential expression of *Crem* mRNA isoforms that include (Tx1, Tx2, Tx4, Tx5, Tx7, Tx9) or exclude (Tx3, Tx6, Tx8, Tx10) exon 4, we examined the numbers of reads mapping to the junctions between exons 3 and 4, 3a and 4, and 3b and 4 (Fig. 3C). RNA-seq data indicated that expression of Tx9 did not differ significantly between wild-type and *Cstf2t*$^{-/-}$ mouse testes. However, reads representing Tx7 were 2.2-fold down-regulated in testes of *Cstf2t*$^{-/-}$ mice (Fig. 3C). Transcripts skipping exon 4 were down-regulated in all three variants analyzed (Tx1, Tx7, Tx9) in *Cstf2t*$^{-/-}$ mice (Fig. 3E).

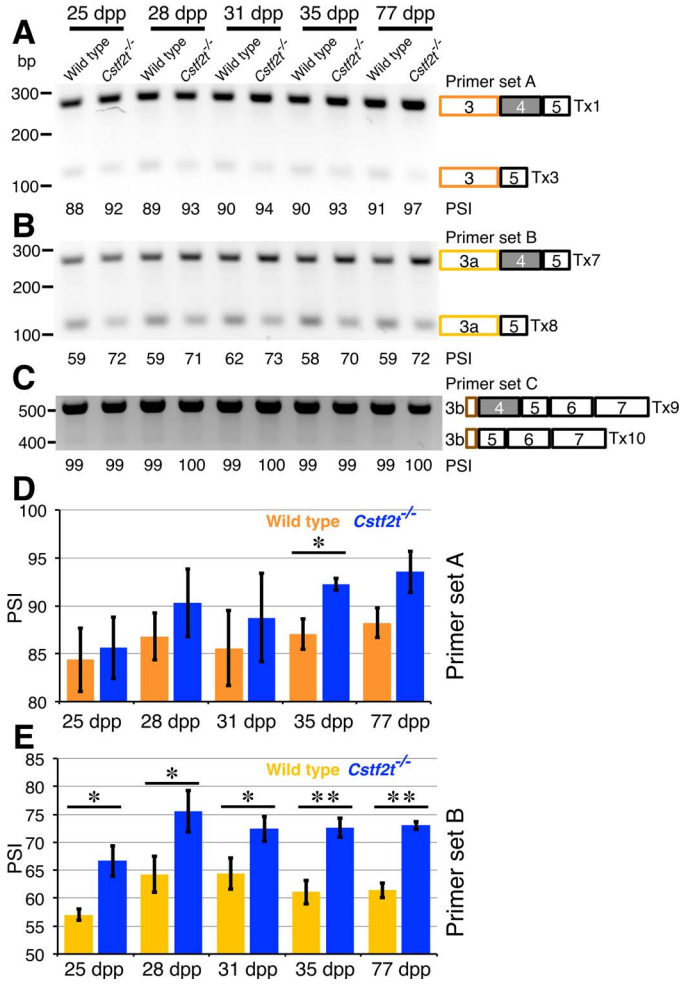

FIG. 4. *Crem* exon 4 is excluded in wild-type but not *Cstf2t*$^{-/-}$ mouse seminiferous tubules. **A**) Agarose gel electrophoresis of PCR products obtained using primer set A for Tx1 (including exon 4) and Tx3 (excluding exon 4) in wild-type and *Cstf2t*$^{-/-}$ mice at 25, 28, 31, 35, and 77 dpp. PSI values calculated from the scanned gel are shown under each lane. DNA size marker is indicated on the left. **B**) Gel electrophoresis of PCR amplified Tx7 (including exon 4) and Tx8 (excluding exon 4) using primer set B in wild-type and *Cstf2t*$^{-/-}$ mice at indicated ages. PSI values are shown under each lane. **C**) Agarose gel electrophoresis of PCR products of Tx9 (including exon 4) and Tx10 (excluding exon 4) using primer set C wild-type and *Cstf2t*$^{-/-}$ mice at indicated ages. PSI values are shown under each lane. **D** and **E**) Densitometry of the PSI values from primer set A (**D**) and primer set B (**E**). Copy DNA quantitation was previously determined in qRT-PCR as in Figures 2 and 5. A single asterisk (*) denotes $P < 0.05$, and two asterisks (**) denote $P < 0.01$ by a one-tailed Student *t*-test of three separate animals of each genotype.

Tx8 (which excludes exon 4) was 4.6-fold reduced in testes from the knockout mice ($P < 0.05$; Fig. 3E).

To validate the RNA-seq results, we used RT-PCR to determine relative exclusion or inclusion of exon 4 in *Crem* transcript variants in wild-type and *Cstf2t*$^{-/-}$ mice at different ages (Fig. 4). Primers were designed to amplify *Crem* mRNA between exons 3 and 5 (primer set A), 3a and 5 (primer set B), or 3b and 7 (primer set C). Using primer set A, we determined the PSI for exon 4 in *Crem* transcripts that initiated from promoter P1 in both wild-type and *Cstf2t*$^{-/-}$ mice (Fig. 4, A and D). PSI values for *Crem* transcripts were similar in *Cstf2t*$^{-/-}$ mice compared to wild type at every age, suggesting little exclusion of exon 4 from transcripts initiating upstream of exon 3 in the *Cstf2t*$^{-/-}$ mice.

With primer set B, we saw smaller PSI values than with primer set A (Fig. 4, B and E). This was consistent with exon 4 exclusion from exon 3a (initiating at promoter P3). PSI values for primer set B in *Cstf2t*$^{-/-}$ mice were also consistently greater than in wild-type mice. This finding agrees with the decrease of reads in the knockout mice skipping exon 4 (Fig. 3E). Because exon exclusion is observed for all transcripts initiating at exon 3a, this further suggests that the feature or features regulating exon 4 inclusion/exclusion are downstream of exon 3a (Fig. 3).

Amplification of mRNA between exon 3b and 7 (primer set C) showed almost no alternative splicing between exons 3b, 4, and 5 in either wild-type or *Cstf2t*$^{-/-}$ mice (Fig. 4C). The relatively small size of the intron that separates exon 3b (whose transcription initiates at P4) and exon 4 may preclude it from participating in alternative splicing of exon 4.

Alternative Splicing of Crem *Does Not Involve Altered Expression of Known Splicing Factors*

Alternative splicing of *Crem* has been studied in cell lines representing male germ cells and other tissues, and these events are under the control of specific splicing factors [15–18]. Thus, two models could account for τCstF-64-dependent exon 4 skipping in mouse testes: 1) τCstF-64 could affect expression of specific splicing factors that in turn control *Crem* exon 4 inclusion or exclusion, or 2) τCstF-64 could bind directly to *Crem* pre-mRNA to enhance exon 4 exclusion (probably in concert with other splicing factors). We first tested the expression of several splicing factors that have been reported to control splicing of *Crem* exons 4 and 7 [15–18]. Using antibodies recognizing either SRp38/NSSR1 (*Srsf10*), SRp40 (*Srsf5*), or DAZ associated protein 1 (*Dazap1*), we performed immunoblots on seminiferous tubule lysates from 25-dpp wild-type and *Cstf2t*$^{-/-}$ mice. We observed no consistent changes in expression of any of these splicing factors between three wild-type and three *Cstf2t*$^{-/-}$ mice at 25 dpp (Supplemental Figure S2B). This suggests that none of these splicing factors are likely to affect *Crem* splicing due to changes in their protein expression levels.

Our next question was whether τCstF-64 was associated with *Crem* pre-mRNA in the vicinity of exon 4. HITS-CLIP data indicated that τCstF-64 bound to the *Crem* pre-mRNA in several locations within the intron between exons 3 and 4 (Supplemental Figure S2A). Since our previous analysis suggested that transcripts initiating at exon 3a had a greater degree of exon 4 exclusion (Fig. 4B), this eliminated the τCstF-64 HITS-CLIP sites upstream of exon 3a. Thus, the strongest candidate for a direct influence of τCstF-64 on *Crem* alternative splicing is the site approximately 1850 nt downstream of exon 3a (Supplemental Figure S2A). Of interest, this HITS-CLIP site coincides with a long interspersed nuclear element (LINE) repeat within this intron. Our previous studies have shown that LINE expression increases in *Cstf2t*$^{-/-}$ mouse testis [38]. This suggests other roles in addition to polyadenylation for τCstF-64 in male germ cells.

Expression of a Subset of CREM-Regulated Genes Is Altered in Cstf2t$^{-/-}$ *Mice*

Changes in CREM expression in *Cstf2t*$^{-/-}$ mice appeared to alter the ratio between activator and inhibitor CREM isoforms (Fig. 1). Therefore, we investigated the expression of genes that are regulated by CREM in the wild-type and *Cstf2t*$^{-/-}$ mice. From the RNA-seq results, we examined the expression of 58 genes whose promoters were shown to be occupied by CREM in haploid germ cells and down-regulated in *Crem* knockout

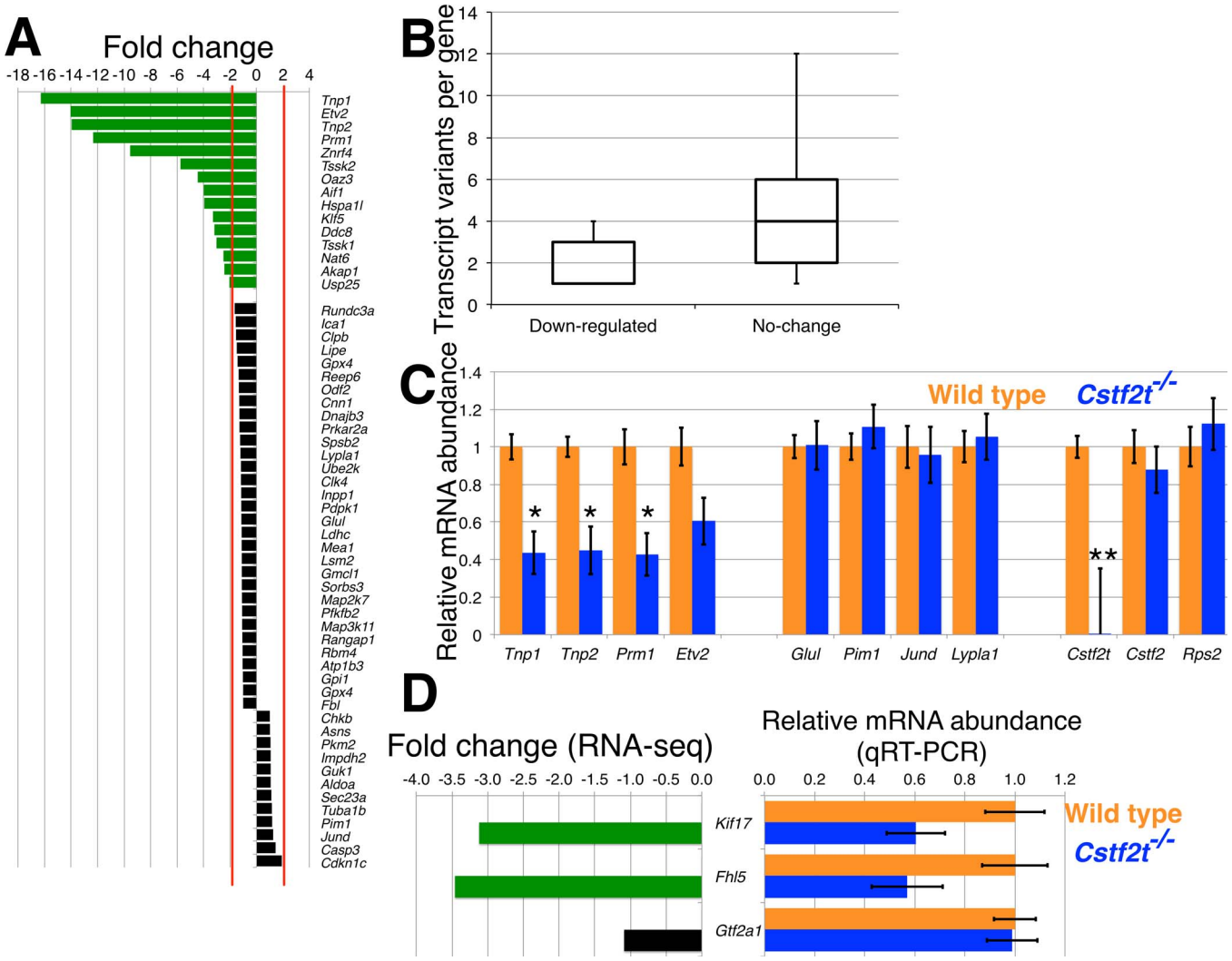

FIG. 5. A subset of CREM-regulated genes is down-regulated in *Cstf2t*$^{-/-}$ mice. **A**) Fold change of CREM-regulated genes [55] in *Cstf2t*$^{-/-}$ versus wild-type seminiferous tubules identified through analysis of RNA-seq data sets. Green bars indicate 2-fold or more down-regulation; black bars indicate no significant change (<2-fold) of mRNA expression. **B**) Median transcript variants number in down-regulated and no change of expression CREM-regulated genes shown using a box-and-whisker plot. The median number of transcript variants for down-regulated genes is one and four for the genes that do not change expression. **C**) Relative mRNA expression of down-regulated genes that are important for spermatogenesis and have a minimum number of transcript variants (panel B, *Tnp1*, *Tnp2*, *Prm1*, *Etv2*) and unchanged genes that have a minimum number of transcript variants (panel B, *Glul*, *Pim1*, *Jund*, *Lypla1*) genes, as well as *Cstf2t*, *Cstf2*, and *Rps2* in wild=type (orange) and *Cstf2t*$^{-/-}$ (blue) testes. A single asterisk (*) denotes $P < 0.05$, and two asterisks (**) denote $P < 0.01$ by a two-tailed Student *t*-test. **D**) Fold change of *Kif17*, *Fhl5* (ACT), and *Gtf2a1* (TFIIA) genes in the *Cstf2t*$^{-/-}$ versus wild-type testes determined using gene expression analysis of RNA-seq data sets (left). Green bars indicate 2-fold or greater down-regulation, and black bar indicates no change. Relative mRNA expression of *Kif17*, *Fhl5* (ACT), and *Gtf2a1* (TFIIA) genes in wild-type (in orange) and *Cstf2t*$^{-/-}$ (in blue) testes as determined by qRT-PCR.

animals [55]. Fifteen of the 58 genes were at least 2-fold down-regulated in testes of 25-dpp *Cstf2t*$^{-/-}$ mice; expression of the remaining genes was relatively unchanged (Fig. 5A). Four down-regulated genes that were important for spermatogenesis and another four that did not change expression were selected for further analysis by qRT-PCR (Fig. 5C). Gene ontology (GO) term analysis [56] of the down-regulated CREM-regulated genes indicated that six genes (*Prm1*, *Tssk1*, *Tssk2*, *Tnp1*, *Tnp2*, *Hspa1l*) were enriched in GO terms for both spermatogenesis (GO term: 0007283, *P*-value, 5.2×10^{-7}, and a false discovery rate [FDR] of 6.1×10^{-4}) and male gamete generation (GO term: 0048232, *P*-value, 5.2×10^{-7}, and FDR, 6.1×10^{-4}). Four of the genes (*Tnp2*, *Prm1*, *Tssk1*, *Tssk2*) are located in two ~10-kb clusters on mouse chromosome 16. No clustering was observed for the genes with unchanged expression. However, we noticed that the down-regulated genes consisted mainly of genes that had a smaller number of transcript variants (taken from the National Center for Biotechnology Information database) due to alternative promoters, splicing, and polyadenylation. The cohort of genes with reduced expression had a median of one transcript per gene, while genes with unchanged expression had a median of four transcript variants per gene (Fig. 5B). This suggests that other mechanisms of transcript regulation, such as intrinsic regulation of genes with only single polyadenylation sites, might be active in testis and in physiological and regulatory clustering of these genes as well as ontological clustering.

In addition, we examined the expression of the CREM-associated gene ACT (*Fhl5*), kinesin family member 17 (*Kif17*), and general transcription factor IIA (*Gtf2a1*) by RNA-seq and qRT-PCR (Fig. 5D). We found that two of these genes, *Kif17* and *Fhl5*, showed decreased mRNA expression in

the *Cstf2t*$^{-/-}$ mice, while *Gtf2a1* did not. This indicates that *Kif17* and *Fhl5* can limit the availability of *Crem* to promoter region of specific genes involved in spermatogenesis, contributing further to the male infertility phenotype of *Cstf2t*$^{-/-}$ mice.

DISCUSSION

τ*CstF-64 Controls* Crem *Polyadenylation in Mouse Testis*

Deletion of *Cstf2t* in mice results in male infertility due to cumulative defects in spermatogenesis and leads to altered expression of thousands of genes [35–38]. We proposed two mechanisms by which τCstF-64 controlled male fertility: 1) a smaller number of genes were affected directly by loss of τCstF-64 (''primary targets''), and 2) a larger number of genes (''secondary targets'') were affected by changes in expression of those primary targets. One primary target of τCstF-64 appears to be the transcriptional regulator *Crem*. To date, neither *CSTF2T* nor *CREM* has been directly implicated in human male infertility [57, 58], although gene deletions in mice have supported both possibilities [35, 49]. Multiple CREM and CREMτ protein isoforms are reduced in testes of *Cstf2t*$^{-/-}$ mice, although some were not affected (Fig. 1). This, combined with CstF-64′s known role in mRNA processing, suggested to us that different *Crem* transcripts were affected differentially by τCstF-64. We identified 11 cleavage/polyadenylation sites in the 3′ exon of the *Crem* gene, of which two were most prominent (Fig. 2A). The proximal site 3 is used most prominently in wild-type mice, while the more distal site 8 is most prominent in *Cstf2t*$^{-/-}$ mice (Fig. 2B). Shortening of the 3′ UTR of *Crem* occurs during male germ cell development in mice between 13 and 14 dpp [19], coincident with the appearance of τCstF-64 [32]. This suggests that the appearance of τCstF-64 in pachynema, the stage of meiotic prophase prior to spermiogenesis, is a significant contributor to the developmental shift in *Crem* polyadenylation and thus controls CREM protein isoforms necessary for spermiogenesis. Further, the developmental switch of *Crem* toward a shorter 3′ UTR reportedly eliminates AUUUA destabilizing elements, increasing the stability of the *Crem* mRNA [19]. A shorter 3′ UTR would also eliminate a conserved miR206/613 binding site [59]. Thus, we propose that major forms of *Crem* mRNA are less stable in *Cstf2t*$^{-/-}$ mice, accounting for overall decreased CREMτ1/2 protein isoforms (Fig. 1).

HITS-CLIP did not identify unique τCstF-64 binding sites in the 3′ exon of *Crem*, although it identified RNA sites that were bound to both τCstF-64 and CstF-64 (Fig. 2A). Thus, we cannot distinguish possible contributions of τCstF-64 from those of CstF-64. Furthermore, these sites were ~150 nt downstream of the distal site and more than 800 nt downstream of the proximal site. This suggested that polyadenylation of *Crem* does not correlate directly with nearby binding of τCstF-64. Other studies have similarly shown that only a subset of polyadenylation sites are correlated with CstF-64 [60] or τCstF-64 [61] binding in HeLa cells.

To explain this, the model that we favor is that τCstF-64 (and, by extension, CstF-64) is dispensable for cleavage and polyadenylation of many genes. The role for τCstF-64 is instead in directing polyadenylation site choice; in its absence, polyadenylation sites are chosen by other default termination mechanisms [62–64]. We favor this model for several reasons. Early in vitro studies showed that CstF enhanced polyadenylation of ''strong'' sites [65] but was less important for ''weak'' sites [66]. Knockdown [50, 61, 67] and knockout [34, 35, 38] studies of both CstF-64 and τCstF-64 have shown that each, while critical for cellular growth and development, was not necessary for expression of most genes. In further support of this model, we note that spermatogenesis, while greatly impaired in testes of *Cstf2t*$^{-/-}$ mice, still produces a few motile spermatozoa [36, 37]. This demonstrates that gene expression is compromised but not arrested in male germ cells in the absence of τCstF-64-mediated polyadenylation. Similarly, embryonic stem cells lacking CstF-64 are able to differentiate into some developmental cell types but not others [68], suggesting that some but not all gene products require CstF-64 for their expression.

The A-seq technique allows us to assign exact sites of poly(A) addition in the 3′ exon. Thus, in further support of the role of τCstF-64 in directing polyadenylation site choice, we note that loss of τCstF-64 results in spreading of the frequency of the A-seq signal across a broader range of sites—''defocusing'' (see Fig. 2C). Defocusing resembles an effect of CstF-64 reported earlier on the SV40 late polyadenylation signal, wherein the site of polyadenylation bifurcated as the CstF binding site was moved distally [30]. However, we cannot explain how defocusing in the *Crem* 3′ exon occurs with the lack of evidence for τCstF-64 binding at the GU-rich DSE at this polyadenylation site (pA#3; Fig. 2C). Defocusing might be evidence supporting the default role of termination in mRNA 3′ end formation in *Cstf2t*$^{-/-}$ mice. However, we have not ruled out other models, including that the absence of τCstF-64 results in structural changes in the CstF or CPSF complexes that alter functions at the cleavage site, even in the absence of a measurable binding site for τCstF-64. Similar structural changes occur in the histone mRNA 3′ end complex in the absence of CstF-64 [34], lending support to this model.

Alternative Splicing of Crem *in* Cstf2t$^{-/-}$ *Mice*

More unexpectedly, loss of τCstF-64 in *Cstf2t*$^{-/-}$ mouse testes altered the splicing of *Crem*, specifically by reducing exclusion of exon 4. Exon 4 encodes a glutamine-rich, Q1 domain that interacts with ACT, a potent transcriptional activator [11–13]. The interaction between CREMτ and ACT bypasses the requirement for a phosphorylation of the P-box domain of CREMτ by PKA and facilitates the activator function of CREMτ on transcription in male germ cells [9, 69]. We propose that τCstF-64 mediates the exclusion of the Q1 domain of CREMτ (which includes exon 4), forming CREMτ1/2 (which exclude exon 4). Thus, splicing-mediated reductions in CREMτ1/2 contribute to the male infertility in *Cstf2t*$^{-/-}$ mice.

The mechanism of τCstF-64′s involvement in exclusion of exon 4 is not yet clear. The reduction is greater in transcripts initiating at promoter P3 (exon 3a; Fig. 3A) than in transcripts initiating at P1 or P4. The exclusion of exon 4 might be due to τCstF-64 effects on other splicing factors. However, expression of two serine/arginine-rich splicing factors, SRp38/NSSR1 (*Srsf10*) and SRp40 (*Srsf5*), and deleted in azoospermia-associated protein 1 (*Dazap1*), reported to participate in regulation of the alternative splicing of *Crem* mRNA, is unchanged between wild-type and *Cstf2t*$^{-/-}$ mice (Supplementary Figure S2B). This suggests that other splicing factors might be involved or that splicing of *Crem* mRNA may be dependent on direct interaction of τCstF-64 with nascent *Crem* mRNAs. The *Crem* transcripts initiating in P3/exon 3a (Tx7 and 8; Fig. 3) are the most affected by the alternative splicing of exon 4 (Fig. 4). We identified a unique HITS-CLIP site for τCstF-64 ~1850 nt downstream of exon 3a (Supplemental Figure S2A). Therefore, it is plausible that direct binding of τCstF-64 to the nascent mRNA of *Crem* (probably in cooperation with other spliceosomal factors) regulates exclu-

sion of exon 4. Future experiments will detail the role of τCstF-64 in alternative splicing of the *Crem* gene.

τCstF-64 Regulates CREM, Which Further Modulates Transcription of Genes Required for Male Germ Cell Development

During spermatogenesis, CREM and its isoforms regulate spatial and temporal expression of male germ-specific genes to ensure development of mature spermatozoa [8, 10]. Mice lacking *Crem* show complete male infertility characterized by azoospermia, reduced seminiferous tubule diameter, and severely impaired spermatogenesis [49]. Similarly, τCstF-64-ablated mice demonstrate infertility with impaired spermatogenesis [35, 36]. The reduced expression of CREMτ2 in testes of *Cstf2t*$^{-/-}$ mice (Fig. 1) led us to test whether expression of genes regulated by CREM was also reduced. However, of 58 CREM-regulated genes [55], 15 were reduced in *Cstf2t*$^{-/-}$ mice (Fig. 5A), while no genes showed significantly increased expression. As an explanation, we note that the ratio between activator and repressor isoforms of CREM is altered in *Cstf2t*$^{-/-}$ mice, resulting in complex effects on downstream gene expression. The 15 down-regulated genes were specifically involved in male gamete formation and development, supporting a deeper role for τCstF-64 in control of spermatogenesis via involvement with CREM.

The reduction in expression of genes regulated by CREM led us also to examine whether *Fhl5* (ACT), *Kif17*, or *Gtf2a1*, all of which act synergistically with CREM, were affected in *Cstf2t*$^{-/-}$ mice. While expression of *Gtf2a1* was unchanged, expression of *Fhl5 and Kif17* was reduced in *Cstf2t*$^{-/-}$ mice (Fig. 5D), suggesting that proper qualitative and quantitative transport of ACT into the nucleus by kinesin might be disrupted. However, spermatogenesis was not impaired in mice ablated of *Fhl5*, suggesting that other members of the *Fhl5* gene family might compensate for the function of ACT in male germ cells [13, 70]. The function of kinesin 17 as a transport vehicle of the members of the *Fhl* gene family is still important, and down-regulation of expression may influence the availability of CREM to transcription sites. These results suggest that the influence of *Cstf2t* on male fertility ranges beyond direct effects on *Crem* and includes ancillary effects on other genes.

τCstF-64 is important for spermatogenesis through several mechanisms. One mechanism is to support the critical balance of *Crem* mRNA isoforms as we explore here. However, there are likely many other critical steps in male germ cell development that are affected as well. For example, previously we determined that loss of τCstF-64 controls testis genome expression [38]. These results are supported by other studies where we show that histone and testis-specific histone-like genes are affected in testes of *Cstf2t*$^{-/-}$ mice (P.N. Grozdanov and C.C. MacDonald, manuscript in preparation). Because *Cstf2t* arose [27, 28] when mammals established sexual dioecy by X- and Y-chromosomal heterogamety [71], it is parsimonious to suggest that many mammalian features of spermatogenesis coevolved to take advantage of its properties to control of germ cell-specific genes and gene isoforms. This fine-tuned control of gene expression would lend special plasticity to mammalian spermatogenesis that is not available in other vertebrate classes. Future studies will examine those mechanisms.

ACKNOWLEDGMENT

The authors thank James L. Manley (Columbia University) for the gift of the anti-SRSF10 antibody, Daniel Webster (Texas Tech University Health Sciences Center) for the gift of the anti-β-tubulin antibody, Shengping Yang for biostatistical consultations, and Jannette Dufour and Laura Reinholdt for insightful comments on the manuscript. Real-time PCR data were generated in the Molecular Biology Core Facility supported in part by TTUHSC.

REFERENCES

1. Hirsh A. Male subfertility. BMJ 2003; 327:669–672.
2. Isidori A, Latini M, Romanelli F. Treatment of male infertility. Contraception 2005; 72:314–318.
3. Matzuk MM, Lamb DJ. The biology of infertility: research advances and clinical challenges. Nat Med 2008; 14:1197–1213.
4. Bhasin S, Mallidis C, Ma K. The genetic basis of infertility in men. Baillières Best Pract Res Clin Endocrinol Metab 2000; 14:363–388.
5. Grootegoed JA, Siep M, Baarends WM. Molecular and cellular mechanisms in spermatogenesis. Baillières Best Pract Res Clin Endocrinol Metab 2000; 14:331–343.
6. Hwang K, Yatsenko AN, Jorgez CJ, Mukherjee S, Nalam RL, Matzuk MM, Lamb DJ. Mendelian genetics of male infertility. Ann N Y Acad Sci 2010; 1214:E1–E17.
7. Idler RK, Yan W. Control of messenger RNA fate by RNA-binding proteins: an emphasis on mammalian spermatogenesis. J Androl 2012; 33: 309–337.
8. Don J, Stelzer G. The expanding family of CREB/CREM transcription factors that are involved with spermatogenesis. Mol Cell Endocrinol 2002; 187:115–124.
9. Kimmins S, Kotaja N, Davidson I, Sassone-Corsi P. Testis-specific transcription mechanisms promoting male germ-cell differentiation. Reproduction 2004; 128:5–12.
10. Hogeveen KN, Sassone-Corsi P. Regulation of gene expression in post-meiotic male germ cells: CREM-signalling pathways and male fertility. Hum Fertil (Camb) 2006; 9:73–79.
11. Fimia GM, Morlon A, Macho B, De Cesare D, Sassone-Corsi P. Transcriptional cascades during spermatogenesis: pivotal role of CREM and ACT. Mol Cell Endocrinol 2001; 179:17–23.
12. Kosir R, Juvan P, Perse M, Budefeld T, Majdic G, Fink M, Sassone-Corsi P, Rozman D. Novel insights into the downstream pathways and targets controlled by transcription factors CREM in the testis. PLoS One 2012; 7: e31798.
13. Lardenois A, Chalmel F, Demougin P, Kotaja N, Sassone-Corsi P, Primig M. Fhl5/Act, a CREM-binding transcriptional activator required for normal sperm maturation and morphology, is not essential for testicular gene expression. Reprod Biol Endocrinol 2009; 7:133.
14. Foulkes NS, Mellstrom B, Benusiglio E, Sassone-Corsi P. Developmental switch of CREM function during spermatogenesis: from antagonist to activator. Nature 1992; 355:80–84.
15. Sanborn BM, Millan JL, Meistrich ML, Moore LC. Alternative splicing of CREB and CREM mRNAs in an immortalized germ cell line. J Androl 1997; 18:62–70.
16. Xiao PJ, Hu L, Li J, Lin W, Chen X, Xu P. NSSR1 is regulated in testes development and cryptorchidism and promotes the exon 5-included splicing of CREB transcripts. Mol Reprod Dev 2007; 74:1363–1372.
17. Tyson-Capper AJ, Bailey J, Krainer AR, Robson SC, Europe-Finner GN. The switch in alternative splicing of cyclic AMP-response element modulator protein CREM$\tau_{2\alpha}$ (activator) to CREMα (repressor) in human myometrial cells is mediated by SRp40. J Biol Chem 2005; 280: 34521–34529.
18. Chen HY, Yu YH, Yen PH. DAZAP1 regulates the splicing of *Crem, Crisp2* and *Pot1a* transcripts. Nucleic Acids Res 2013; 41:9858–9869.
19. Foulkes NS, Schlotter F, Pévet P, Sassone-Corsi P. Pituitary hormone FSH directs the CREM functional switch during spermatogenesis. Nature 1993; 362:264–267.
20. Molina CA, Foulkes NS, Lalli E, Sassone-Corsi P. Inducibility and negative autoregulation of CREM: an alternative promoter directs the expression of ICER, an early response repressor. Cell 1993; 75:875–886.
21. Delmas V, Laoide BM, Masquilier D, de Groot RP, Foulkes NS, Sassone-Corsi P. Alternative usage of initiation codons in mRNA encoding the cAMP-responsive-element modulator generates regulators with opposite functions. Proc Natl Acad Sci U S A 1992; 89:4226–4230.
22. Foulkes NS, Borrelli E, Sassone-Corsi P. CREM gene: use of alternative

DNA-binding domains generates multiple antagonists of cAMP-induced transcription. Cell 1991; 64:739–749.
23. Behr R, Weinbauer GF. CREM activator and repressor isoforms in human testis: sequence variations and inaccurate splicing during impaired spermatogenesis. Mol Hum Reprod 2000; 6:967–972.
24. Nantel F, Monaco L, Foulkes NS, Masquilier D, LeMeur M, Henriksen K, Dierich A, Parvinen M, Sassone-Corsi P. Spermiogenesis deficiency and germ-cell apoptosis in CREM-mutant mice. Nature 1996; 380:159–162.
25. Wallace AM, Dass B, Ravnik SE, Tonk V, Jenkins NA, Gilbert DJ, Copeland NG, MacDonald CC. Two distinct forms of the 64,000 M_r protein of the cleavage stimulation factor are expressed in mouse male germ cells. Proc Natl Acad Sci U S A 1999; 96:6763–6768.
26. Dass B, Attaya EN, Wallace AM, MacDonald CC. Overexpression of the CstF-64 and CPSF-160 polyadenylation protein messenger RNAs in mouse male germ cells. Biol Reprod 2001; 64:1722–1729.
27. Dass B, McDaniel L, Schultz RA, Attaya E, MacDonald CC. The gene CSTF2T encoding the human variant CstF-64 polyadenylation protein τCstF-64 is intronless and may be associated with male sterility. Genomics 2002; 80:509–514.
28. Dass B, McMahon KW, Jenkins NA, Gilbert DJ, Copeland NG, MacDonald CC. The gene for a variant form of the polyadenylation protein CstF-64 is on chromosome 19 and is expressed in pachytene spermatocytes in mice. J Biol Chem 2001; 276:8044–8050.
29. Yan W, McCarrey JR. Sex chromosome inactivation in the male. Epigenetics 2009; 4:452–456.
30. MacDonald CC, Wilusz J, Shenk T. The 64-kilodalton subunit of the CstF polyadenylation factor binds to pre-mRNAs downstream of the cleavage site and influences cleavage site location. Mol Cell Biol 1994; 14: 6647–6654.
31. Monarez RR, MacDonald CC, Dass B. Polyadenylation proteins CstF-64 and τCstF-64 exhibit differential binding affinities for RNA polymers. Biochem J 2007; 401:651–658.
32. Wallace AM, Denison T, Attaya EN, MacDonald CC. Developmental differences in expression of two forms of the CstF-64 polyadenylation protein in rat and mouse. Biol Reprod 2004; 70:1080–1087.
33. MacDonald CC, McMahon KW. Tissue-specific mechanisms of alternative polyadenylation: testis, brain and beyond. WIRES RNA 2010; 1: 494–501.
34. Youngblood BA, Grozdanov PN, MacDonald CC. CstF-64 supports pluripotency and regulates cell cycle progression in embryonic stem cells through histone 3′ end processing. Nucleic Acids Res 2014; 42: 8330–8342.
35. Dass B, Tardif S, Park JY, Tian B, Weitlauf HM, Hess RA, Carnes K, Griswold MD, Small CL, MacDonald CC. Loss of polyadenylation protein τCstF-64 causes spermatogenic defects and male infertility. Proc Natl Acad Sci U S A 2007; 104:20374–20379.
36. Tardif S, Akrofi A, Dass B, Hardy DM, MacDonald CC. Infertility with impaired zona pellucida adhesion of spermatozoa from mice lacking τCstF-64. Biol Reprod 2010; 83:464–472.
37. Hockert KJ, Martincic K, Mendis-Handagama SMLC, Borghesi LA, Milcarek C, Dass B, MacDonald CC. Spermatogenetic but not immunological defects in mice lacking the τCstF-64 polyadenylation protein. J Reprod Immunol 2011; 89:26–37.
38. Li W, Yeh HJ, Shankarling GS, Ji Z, Tian B, MacDonald CC. The τCstF-64 polyadenylation protein controls genome expression in testis. PLoS One 2012; 7:e48373.
39. Shin C, Manley JL. The SR protein SRp38 represses splicing in M phase cells. Cell 2002; 111:407–417.
40. Martin G, Gruber AR, Keller W, Zavolan M. Genome-wide analysis of pre-mRNA 3′ end processing reveals a decisive role of human cleavage factor I in the regulation of 3′ UTR length. Cell Rep 2012; 1:753–763.
41. Grozdanov PN, Macdonald CC. High-throughput sequencing of RNA isolated by cross-linking and immunoprecipitation (HITS-CLIP) to determine sites of binding of CstF-64 on nascent RNAs. Methods Mol Biol 2014; 1125:187–208.
42. Andrews S. FASTQC: A Quality Control tool for High Throughput Sequence Data [Internet]. Cambridge, UK: Babraham Institute. http://www.bioinformatics.babraham.ac.uk/projects/fastqc/. Accessed 5 January 2016.
43. Kent WJ. BLAT—the BLAST-like alignment tool. Genome Res 2002; 12: 656–664.
44. Cunningham F, Amode MR, Barrell D, Beal K, Billis K, Brent S, Carvalho-Silva D, Clapham P, Coates G, Fitzgerald S, Gil L, Giron CG, et al. Ensembl 2015. Nucleic Acids Res 2015; 43:D662–D669.
45. Chen B, Yun J, Kim MS, Mendell JT, Xie Y. PIPE-CLIP: a comprehensive online tool for CLIP-seq data analysis. Genome Biol 2014; 15:R18.
46. Wang Z, Gerstein M, Snyder M. RNA-Seq: a revolutionary tool for transcriptomics. Nat Rev Genet 2009; 10:57–63.
47. Mortazavi A, Williams BA, McCue K, Schaeffer L, Wold B. Mapping and quantifying mammalian transcriptomes by RNA-Seq. Nat Methods 2008; 5:621–628.
48. Livak KJ, Schmittgen TD. Analysis of relative gene expression data using real-time quantitative PCR and the $2^{-\Delta\Delta Ct}$ Method. Methods 2001; 25: 402–408.
49. Blendy JA, Kaestner KH, Weinbauer GF, Nieschlag E, Schutz G. Severe impairment of spermatogenesis in mice lacking the CREM gene. Nature 1996; 380:162–165.
50. Ruepp MD, Schweingruber C, Kleinschmidt N, Schümperli D. Interactions of CstF-64, CstF-77, and symplekin: implications on localisation and function. Mol Biol Cell 2011; 22:91–104.
51. MacDonald CC, Redondo J-L. Reexamining the polyadenylation signal: were we wrong about AAUAAA? Mol Cell Endocrinol 2002; 190:1–8.
52. Tian B, Graber JH. Signals for pre-mRNA cleavage and polyadenylation. Wiley Interdiscip Rev RNA 2012; 3:385–396.
53. Seidl MD, Nunes F, Fels B, Hildebrandt I, Schmitz W, Schulze-Osthoff K, Muller FU. A novel intronic promoter of the Crem gene induces small ICER (smICER) isoforms. FASEB J 2014; 28:143–152.
54. Gellersen B, Kempf R, Sandhowe R, Weinbauer GF, Behr R. Novel leader exons of the cyclic adenosine 3′,5′-monophosphate response element modulator (CREM) gene, transcribed from promoters P3 and P4, are highly testis-specific in primates. Mol Hum Reprod 2002; 8:965–976.
55. Martianov I, Choukrallah MA, Krebs A, Ye T, Legras S, Rijkers E, Van Ijcken W, Jost B, Sassone-Corsi P, Davidson I. Cell-specific occupancy of an extended repertoire of CREM and CREB binding loci in male germ cells. BMC Genomics 2010; 11:530.
56. Ashburner M, Ball CA, Blake JA, Botstein D, Butler H, Cherry JM, Davis AP, Dolinski K, Dwight SS, Eppig JT, Harris MA, Hill DP, et al. Gene ontology: tool for the unification of biology. The Gene Ontology Consortium. Nat Genet 2000; 25:25–29.
57. Krausz C, Sassone-Corsi P. Genetic control of spermiogenesis: insights from the CREM gene and implications for human infertility. Reprod Biomed Online 2005; 10:64–71.
58. Christensen GL, Wooding SP, Ivanov IP, Atkins JF, Carrell DT. Sequencing and haplotype analysis of the activator of CREM in the testis (ACT) gene in populations of fertile and infertile males. Mol Hum Reprod 2006; 12:257–262.
59. Friedman RC, Farh KK, Burge CB, Bartel DP. Most mammalian mRNAs are conserved targets of microRNAs. Genome Res 2009; 19:92–105.
60. Yao C, Biesinger J, Wan J, Weng L, Xing Y, Xie X, Shi Y. Transcriptome-wide analyses of CstF64-RNA interactions in global regulation of mRNA alternative polyadenylation. Proc Natl Acad Sci U S A 2012; 109:18773–18778.
61. Yao C, Choi EA, Weng L, Xie X, Wan J, Xing Y, Moresco JJ, Tu PG, Yates JR III, Shi Y. Overlapping and distinct functions of CstF64 and CstF64τ in mammalian mRNA 3′ processing. RNA 2013; 109: 18773–18778.
62. Gromak N, West S, Proudfoot NJ. Pause sites promote transcriptional termination of mammalian RNA polymerase II. Mol Cell Biol 2006; 26: 3986–3996.
63. Proudfoot NJ. Ending the message: poly(A) signals then and now. Genes Dev 2011; 25:1770–1782.
64. Andersen PK, Jensen TH, Lykke-Andersen S. Making ends meet: coordination between RNA 3′-end processing and transcription initiation. Wiley Interdiscip Rev RNA 2013; 4:233–246.
65. Takagaki Y, Ryner LC, Manley JL. Four factors are required for 3′-end cleavage of pre-mRNAs. Genes Dev 1989; 3:1711–1724.
66. Weiss EA, Gilmartin GM, Nevins JR. Poly(A) site efficiency reflects the stability of complex formation involving the downstream element. EMBO J 1991; 10:215–219.
67. Takagaki Y, Manley JL. Levels of polyadenylation factor CstF-64 control IgM heavy chain mRNA accumulation and other events associated with B cell differentiation. Mol Cell 1998; 2:761–771.
68. Youngblood BA, MacDonald CC. CstF-64 is necessary for endoderm differentiation resulting in cardiomyocyte defects. Stem Cell Res 2014; 13: 413–421.
69. Fimia GM, De Cesare D, Sassone-Corsi P. CBP-independent activation of CREM and CREB by the LIM-only protein ACT. Nature 1999; 398: 165–169.
70. Kotaja N, De Cesare D, Macho B, Monaco L, Brancorsini S, Goossens E, Tournaye H, Gansmuller A, Sassone-Corsi P. Abnormal sperm in mice

with targeted deletion of the *act* (activator of cAMP-responsive element modulator in testis) gene. Proc Natl Acad Sci U S A 2004; 101: 10620–10625.

71. Bachtrog D, Kirkpatrick M, Mank JE, McDaniel SF, Pires JC, Rice W, Valenzuela N. Are all sex chromosomes created equal? Trends Genet 2011; 27:350–357.